DOI: 10.1002/cctc.201301063

Ethylene Polymerization Catalyzed by Pyrene-Tagged Iron Complexes: The Positive Effect of π-Conjugation and Immobilization on Multiwalled Carbon Nanotubes

Liping Zhang,[a, b] Wenjuan Zhang,[b] Philippe Serp,[a] Wen-Hua Sun,*[b] and Jérôme Durand*[a]

2-[1-(2,6-Diisopropylphenylimino)ethyl]-6-[1-(pyren-1-ylimino)-ethyl]pyridine (**L1**) and 2,6-bis[1-(pyren-1-ylimino)ethyl]pyridine (**L2**) were synthesized and used to prepare the corresponding Fe complexes **Fe1** and **Fe2** from $FeCl_2$. All new compounds were characterized, and single-crystal XRD analysis of **Fe1** was performed. The π-conjugated pyrenyl substituent enhanced the catalytic activity of the Fe complexes, which display high activity in ethylene polymerization up to $10^7\,g_{PE}\,mol_{Fe}^{-1}\,h^{-1}$ (PE = polyethylene). These Fe complexes were easily immobilized on multiwalled carbon nanotubes (MWCNTs) through noncovalent π–π interactions. The supported precatalysts showed better ethylene polymerization activity than their homogeneous counterparts to produce well-dispersed MWCNT/PE composite materials.

Introduction

Multiwalled carbon nanotubes (MWCNTs) exhibit a number of attractive features, such as good electronic and thermal conductivity, which have led to important applications in various fields of chemical and material sciences over the last few years.[1] In spite of the growing interest generated by carbon nanotubes (CNTs) as a support in catalytic applications,[2] reports on the immobilization of discrete single-site transition-metal-based catalysts remain scarce.[3–9] Among these reports, some mention the beneficial influence of carbon nanomaterials on the performances of early-transition-metal-based olefin polymerization catalysts.[4] In particular, a combination of steric and electronic effects can result in an increased molecular weight for polyethylene (PE) produced by MWCNT/metallocene,[5] MWCNT/half-titanocene,[6] or MWCNT/Ziegler–Natta[7] catalytic systems. Recently, we reported the positive influence of CNTs or graphene immobilized Ni-based catalysts on ethylene polymerization.[8] Nanoparticle-supported catalysts efficiently produced PE nanocomposites and allowed good levels of dispersion and/or improved physical properties.[7,9]

At the end of last century, a series of iron and cobalt complexes with bulky 2,6-bis(imino)-pyridine ligands applied to olefin polymerization have been discovered by Brookhart[10] and Gibson[11] Since then, the late transition metal complexes for ethylene activation have attracted increased attention, both in academic and industrial research.[12] Subsequently, the 2,6-bis(imino)pyridine ligand framework has become the subject of extensive investigations.[13] The corresponding catalysts highlighted the important role of the synergy between steric and electronic effects of the ligands and the catalytically active metal center. Immobilization of such iron catalysts on various inorganic supports has been carried out, resulting most of the time in a reduced catalytic activity compared to the unsupported system[14] with only few examples where high activity is maintained after immobilization.[15]

If we consider their good electron conductivity and bulkiness, CNTs can be a good candidate as macroligands to control the electronic and steric influences on the reactivity of CNT-immobilized late-transition-metal precatalysts in ethylene polymerization. Moreover, the good thermal conductivity of MWCNTs provides thermostability to the linked molecular species; therefore, the CNT-immobilized complex precatalysts maintain, during the highly exothermic polymerization reaction, a better temperature parameter and hence enhanced activities. The anchoring of molecular species through π–π interactions between the graphitic surface and a polyaromatic group[16] allows the stacking of conjugated molecules on the intact CNT surface, which maintains its conductive properties.[17] Moreover, the straightforward π–π interactions afforded efficient immobilization to avoid common covalent functionalization that requires preliminary chemical modification of the CNT surface.[18] To perform noncovalent immobilization of complexes on CNTs, a pyrene motif is seen as a valuable and elegant approach.[2d,3g,k,n]

Although CNT-supported Fe complexes have already been reported for other catalytic reactions,[19] there is, to the best of our knowledge, no report that deals with ethylene polymerization by CNT-immobilized Fe precatalysts. Pyrene-tagged 2,6-bis(imino)pyridine derivatives were synthesized and used

---

[a] *L. Zhang, Prof. P. Serp, Dr. J. Durand*
Laboratoire de Chimie de Coordination UPR CNRS 8241
composante ENSIACET
Université de Toulouse
4 allée Emile Monso-CS 44362, 31030 Toulouse Cedex 4 (France)
Fax: (+33) 534323596
E-mail: jerome.durand@ensiacet.fr

[b] *L. Zhang, Dr. W. Zhang, Prof. W.-H. Sun*
Key laboratory of Engineering Plastics
and Beijing National Laboratory for Molecular Science
Institute of Chemistry, Chinese Academy of Sciences
Beijing 100190 (China)
E-mail: whsun@iccas.ac.cn

to form their Fe complexes, which were immobilized onto MWCNTs through π stacking. All these Fe complexes showed high activities, in both homogenous and heterogeneous manners, towards ethylene polymerization, in which the CNT-immobilized precatalysts can exhibit even higher activity. Herein the synthesis and characterization of these complexes and their immobilization on MWCNTs are reported as well as their performances in ethylene polymerization.

Results and Discussion

Synthesis and characterization of ligands and Fe complexes

The pyrene-tagged 2,6-bis(arylimino)pyridine derivatives 2-[1-(2,6-diisopropylphenylimino)ethyl]-6-[1-(pyren-1-ylimino)ethyl]-pyridine (**L1**) and 2,6-bis[1-(pyren-1-ylimino)ethyl]pyridine (**L2**) were synthesized according to a procedure reported previously[13a,h] (Scheme 1). **L1** and **L2** reacted individually with a molar equivalent of $FeCl_2$ in THF to afford the corresponding Fe complexes **Fe1** and **Fe2** in high yields (Scheme 1). All organic and complex compounds are air stable, however, the solutions of the Fe complexes turn slowly from blue to yellow in air, which indicates the oxidation of iron(II) to iron(III). All compounds were characterized. In comparison to the IR spectra of **L1** and **L2**, the C=N stretching vibrations in the spectra of **Fe1** and **Fe2** are shifted to lower frequencies (1586 vs. 1639 and 1638 cm^{-1}), which indicates effective coordination between the imino N atoms and the Fe center. The molecular structure of **Fe1** was further confirmed by single-crystal XRD analysis (Figure 1).

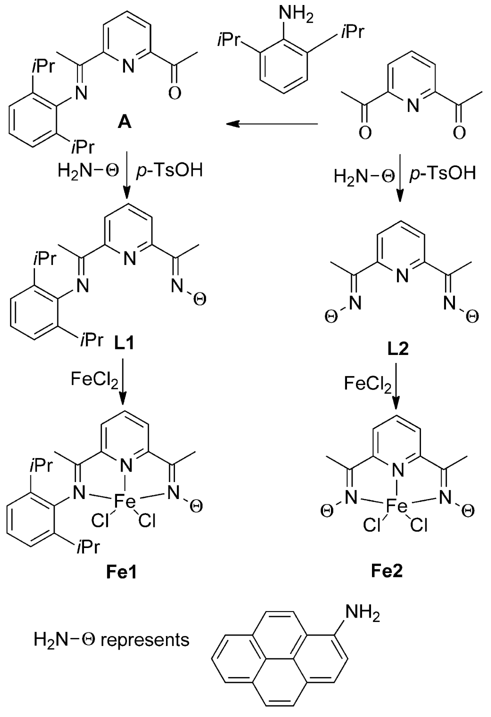

Scheme 1. Synthetic procedure for **L1**, **L2**, **Fe1**, and **Fe2**.

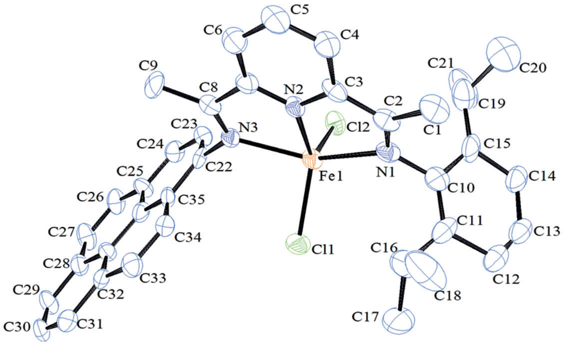

Figure 1. ORTEP representation of the molecular structure of **Fe1**. Thermal ellipsoids are shown at 30% probability. H atoms have been omitted for clarity. Selected bond lengths [Å] and angles [°]: Fe1–N1 2.296(5), Fe1–N2 2.083(4), Fe1–N3 2.247(5), Fe1–Cl1 2.2723(18), Fe1–Cl2 2.3000(19), N1–Fe1–N2 73.28(19), N1–Fe1–N3 146.22(19), N2–Fe1–N3 73.05(17), Cl1–Fe1–Cl2 115.82(7).

The coordination geometry of the Fe center could be described as distorted square-pyramidal, with the basal plane composed of N1, N2, N3, and Cl1. The Fe center deviates from the basal plane by 0.6574 Å, and Cl2 deviates by 2.9465 Å on the same side. The equatorial plane formed by N1, N2, and N3 is almost perpendicular to the imino-pyrene ring (86.1°) and to the 2,6-diisopropylphenyl group (79.1°). Two Cl locate on the different sites from the basal plane at a distance of 1.6508 Å for Cl1 and 2.1830 Å for Cl2. With regard to the bond lengths around the Fe center, Fe1–Cl2 (2.3000(19) Å) is longer than Fe1–Cl1 (2.2723(18) Å); the Fe1–N1 bond length is similar to that of Fe1–N3 but longer than that of Fe1–N2 (≈0.2 Å). This is partly because N1 and N3 belong to imino groups and N2 belongs to the pyridine ring. A similar geometry was also observed for analogous tridentate iron(II) complexes.[10b,11b,13e–g,20]

The immobilization of **Fe1** and **Fe2** on MWCNTs was then performed under a N_2 atmosphere by stirring a CH_2Cl_2 solution that contained the appropriate complex and a suspension of the purified CNTs (Scheme 2). The suspension was collected by filtration and washed with toluene and CH_2Cl_2 several times until the filtrate was colorless. X-ray photoelectron spectroscopy (XPS) confirmed the presence of only Fe^{II} species on the MWCNT surface without peaks that correspond to Fe^0, indicative of the stability of the Fe complexes during the anchoring process. As a result of the deviation within semiquantitative analysis by XPS, the exact amount of Fe immobilized on the MWCNTs was determined by using inductively coupled plasma mass spectrometry (ICP-MS; 2658 $mg_{Fe}\,kg^{-1}$ for **Fe1** and 2909 $mg_{Fe}\,kg^{-1}$ for **Fe2**).

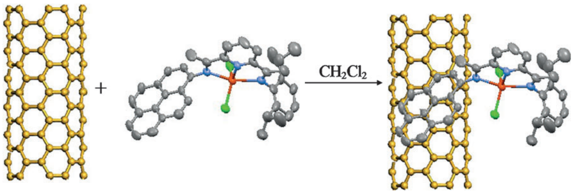

Scheme 2. Schematic representation of the immobilization of **Fe1** on MWCNTs.

Table 1. Ethylene polymerization with **Fe1** and **Fe2** precatalysts.[a]

Entry	Catalyst	Cocatalyst	Al/Fe	T [°C]	t [min]	PE [g]	Activity[b]	T_m[c] [°C]	M_w[d] [kg mol^{-1}]	M_w/M_n[d]
1	**Fe1**	MAO	1000	30	30	5.7	2.3	128.7	108	80.3
2	**Fe1**	MMAO	1000	30	30	10.5	4.2	124.6	21.6	10.2
3	**Fe1**	MMAO	1500	30	30	15.9	6.4	124.7	16.3	9.30
4	**Fe1**	MMAO	2000	30	30	19.8	7.9	124.4	30.4	19.8
5	**Fe1**	MMAO	2500	30	30	17.3	7.0	124.2	39.5	30.9
6	**Fe1**	MMAO	3000	30	30	15.3	6.1	125.3	n.d.	n.d.
7	**Fe1**	MMAO	2000	40	30	16.7	6.7	122.1	38.1	22.4
8	**Fe1**	MMAO	2000	50	30	13.8	5.5	127.6	112	75.6
9	**Fe1**	MMAO	2000	30	5	11.4	27.4	122.4	4.32	2.40
10	**Fe1**	MMAO	2000	30	10	13.4	16.1	123.8	14.1	7.50
11	**Fe1**	MMAO	2000	30	15	15.2	12.2	124.0	12.4	8.20
12	**Fe1**	MMAO	2000	30	45	21.3	5.7	125.8	71.2	66.5
13	**Fe1**	MMAO	2000	30	60	22.8	4.6	125.1	38.8	32.2
14	**Fe2**	MMAO	1500	30	30	23.7	9.5	120.1	3.57	2.9
15	**Fe2**	MMAO	2000	30	30	28.9	11.5	119.9	2.71	3.0
16	**Fe2**	MMAO	2500	30	30	22.3	8.9	119.5	3.38	4.1
17	**Fe2**	MMAO	2000	40	30	15.5	6.2	122.0	4.39	3.3
18	**Fe2**	MMAO	2000	50	30	13.6	5.4	122.7	6.12	5.1

[a] Reaction conditions: 5 μmol of Fe; 10 atm ethylene; 100 mL toluene. [b] $10^6\ g_{PE}\,mol_{Fe}^{-1}\,h^{-1}$. [c] Determined by DSC. [d] Determined by GPC.

Ethylene polymerization by the Fe complexes

To both optimize the polymerization parameters and evaluate the pyrene-induced influence of the ligands, precatalyst **Fe1** was explored under various conditions under 10 atm of ethylene (Table 1). With regard to the different efficiency of cocatalysts, methylaluminoxane (MAO) and modified methylaluminoxane (MMAO) were tested (Table 1, Entries 1–2), and MMAO was the best activator (Table 1, Entry 2), which was further used in the catalytic systems. If we varied the Al/Fe molar ratio from 1000 to 3000 (Table 1, Entries 2–6), the best activity was achieved at Al/Fe 2000 (Table 1, Entry 4). The molecular weight (M_w) and polydispersity (M_w/M_n) values of the obtained PE gradually increased along with the molar Al/Fe ratio (Table 1, Entries 3–5). The catalytic activity decreased slightly if the reaction temperature was elevated from 30 to 50 °C (Table 1, Entries 4, 7, 8), due to the lower concentration of ethylene at a higher temperature. Surprisingly, the molecular weights and the molecular polydispersity of PE were slightly increased at higher temperatures (M_w from 30.4–127.6 kg mol^{-1} and M_w/M_n from 19.8–75.6). The higher molecular weight of the obtained PE provided information on stable intermediates during polymerization; therefore, the catalytic system has better thermostability at an elevated reaction temperature. With regard to the lifetime of the active species (Table 1, Entries 4, 9–12), the highest value of $2.74\times10^7\ g_{PE}\,mol_{Fe}^{-1}\,h^{-1}$ was observed within 5 min (Table 1, Entry 9), and the polymerization was almost finished after 30 min (catalytic activity of $7.9\times10^6\ g_{PE}\,mol_{Fe}^{-1}\,h^{-1}$; Table 1, Entry 4).

Subsequently, the precatalyst **Fe2** was also explored by using MMAO as the cocatalyst (Table 1, Entries 14–18), which confirmed the optimal Al/Fe molar ratio of 2000 at 30 °C (Table 1, Entry 15). Meanwhile, the activity was $1.15\times10^7\ g_{PE}\,mol_{Fe}^{-1}\,h^{-1}$ (Table 1, Entry 15), which makes **Fe2** approximately 1.5 times more active than **Fe1** (Table 1, Entry 4). In addition, compared to the properties of the PEs obtained by using **Fe1**, the M_w and M_w/M_n values of the PEs obtained by using **Fe2** are less sensitive to the polymerization temperature (Figure 2). The narrower molecular polydispersity of the obtained PEs can probably be attributed to the symmetric structure of the **Fe2** precatalyst.

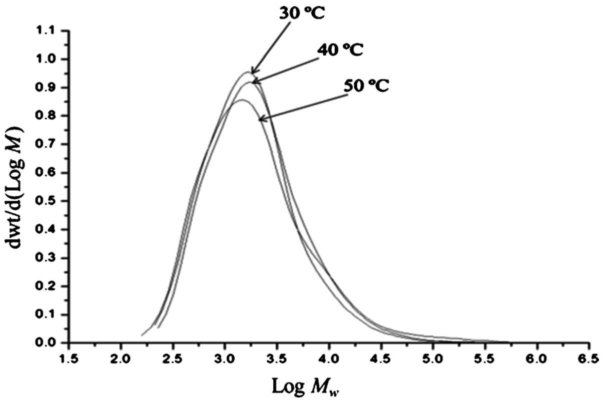

Figure 2. GPC curves of PE produced by **Fe2** at different temperatures (Entries 15, 17, and 18 in Table 1).

According to the observed data, the current complex precatalysts generally showed higher activities than their analogs,[10a, 11, 21] which illustrates the positive influence of the pyrene-tagged ligands on the Fe complexes. PEs with lower molecular weights were reported by using Fe complexes that bear ligands that lack *ortho*-substituted aryl groups;[10b, c, 11d, 13g] although there is no substituent on 1-aminopyrene, the current precatalysts produced PEs with higher molecular weights than their analogues. The pyrene motif played an important role as a bulky aryl group, which was confirmed by the replacement of the 2,6-diisopropylphenyl moiety that forms **Fe1** by a pyrene fragment within **Fe2** to result in a higher activity in ethylene polymerization.

Polymerization using the MWCNT-supported Fe precatalysts

Subsequently, the polymerization behavior of MWCNT-supported Fe precatalysts was conducted in the presence of MMAO. The influence of the reaction parameters, which include the Al/Fe molar ratio and reaction temperature, was studied by using the MWCNT-**Fe1**/MMAO system. Upon increasing the Al/Fe ratio from 1500 to 4000 (Table 2, Entries 1–5), the activity increased sharply to reach a maximum at Al/Fe = 3000. This optimum ratio for the MWCNT-supported Fe precatalyst is significantly higher than that of the corresponding homogenous catalyst (vide supra). The high MMAO consumption can be attributed to the interaction force between the CNTs and the Fe complex that requires a larger amount of cocatalyst for activation and/or because some of the cocatalyst is adsorbed on the CNT surface. On the other hand, the best catalytic activity was reached by the MWCNT-**Fe1** system after 30 min ($9.11\times 10^6\ g_{PE}\,mol_{Fe}^{-1}\,h^{-1}$), which was not only higher than that of the homogeneous **Fe1** system (Table 2, Entry 3 vs. Table 1, Entry 4) but also evidenced a beneficial influence of the MWCNT to result in a better stability. Charge transfer between the CNTs and various adsorbed species was reported in the literature,[22] which includes an example of immobilized precatalysts in ethylene polymerization.[9c]

In the experiments with various Al/Fe molar ratios, the PEs obtained by the MWCNT-**Fe1** system showed adaptable molecular weights ($M_w = 5.07$–$27.6\ kg\,mol^{-1}$), with narrower molecular polydispersity ($M_w/M_n = 2.2$–12.1) than that of the homogeneous system. However, the best activity for MWCNT-**Fe2** was $8.35\times 10^6\ g_{PE}\,mol_{Fe}^{-1}\,h^{-1}$ (Table 2, Entry 9), which was lower than that of its corresponding homogeneous counterpart (Table 1, Entry 15). Two pyrene rings are present within the framework of **Fe2**, both of which could interact with the MWCNTs surface to result in a too high steric hindrance around the Fe center and, therefore, lead to a lower activity compared to its unsupported counterpart.

The optimum molar ratio of Al/Fe (3000) was used to investigate the influence of the reaction temperature (Table 2, Entries 3, 6, and 7 for MWCNT-**Fe1** and Entries 9, 11, and 12 for MWCNT-**Fe2**). The elevated reaction temperature resulted in a lower catalytic activity, even more pronounced in the case of the supported systems, which evidences that the MWCNTs are not able to stabilize the active species at higher temperatures because of weak π–π interactions. Moreover, the M_w and M_w/M_n values are also influenced by the temperature: higher molecular weights and broader distributions are observed at elevated reaction temperatures for MWCNT-**Fe1** (Figure 3).

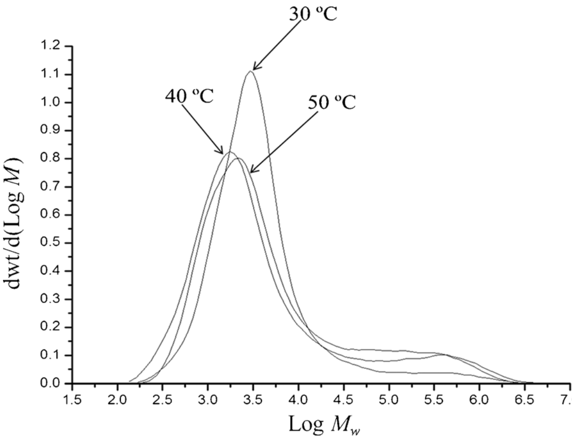

Figure 3. GPC traces of PE produced by MWCNT-supported **Fe1** at different temperatures (Entries 3, 6, and 7 in Table 2).

Interestingly, the M_w and M_w/M_n values for the PE obtained by using MWCNT-**Fe2** decrease slightly at higher reaction temperatures because two pyrene groups are available to interact with the MWCNTs. One advantage was the production of PEs with a narrow polydispersity (Figure 4). This phenomenon is opposite to the trend observed for MWCNT-**Fe1**.

During the polymerization process, PE nanocomposites were formed by the direct growth of the polymeric chains from the MWCNTs surface as a result of its interaction with the catalytically active species. Surface-initiated polymerization processes have been reported in some cases as an efficient way to disperse CNTs into PE matrices homogeneously.[6–9]

The polymeric materials obtained by using MWCNT-supported Fe catalysts were analyzed by SEM and TEM, which evidenced a good level of dispersion inside the PE matrix of the individually separated MWCNTs (Figure 5 a). If some of the

Table 2. Ethylene polymerization with MWCNT-**Fe*x*** precatalysts/MMAO.[a]

Entry	Catalyst	Al/Fe	T [°C]	t [min]	PE [g]	Activity[b]	T_m[c] [°C]	M_w[d] [kg mol^{-1}]	M_w/M_n[d]
1	MWCNT/**Fe1**	1500	30	30	3.8	3.21	124.4	18.8	12.1
2	MWCNT/**Fe1**	2500	30	30	5.4	4.57	124.0	6.59	3.50
3	MWCNT/**Fe1**	3000	30	30	10.8	9.11	126.4	27.6	12.6
4	MWCNT/**Fe1**	3500	30	30	6.7	5.65	124.8	5.07	2.20
5	MWCNT/**Fe1**	4000	30	30	5.1	4.30	123.7	18.6	11.2
6	MWCNT/**Fe1**	3000	40	30	6.2	5.23	127.5	55.5	23.6
7	MWCNT/**Fe1**	3000	50	30	2.4	2.03	127.9	67.9	27.2
8	MWCNT/**Fe2**	2500	30	30	7.41	5.70	122.4	11.5	8.48
9	MWCNT/**Fe2**	3000	30	30	10.86	8.35	122.4	8.32	5.61
10	MWCNT/**Fe2**	4000	30	30	5.38	4.14	122.9	8.76	6.29
11	MWCNT/**Fe2**	3000	40	30	6.03	4.64	121.0	4.13	2.99
12	MWCNT/**Fe2**	3000	50	30	2.58	1.98	122.2	3.88	2.38

[a] Reaction conditions: 0.05 g of MWCNT-**Fe*x***; 10 atm ethylene; 100 mL toluene. [b] $10^6\ g_{PE}\,mol_{Fe}^{-1}\,h^{-1}$. [c] Determined by DSC. [d] Determined by GPC.

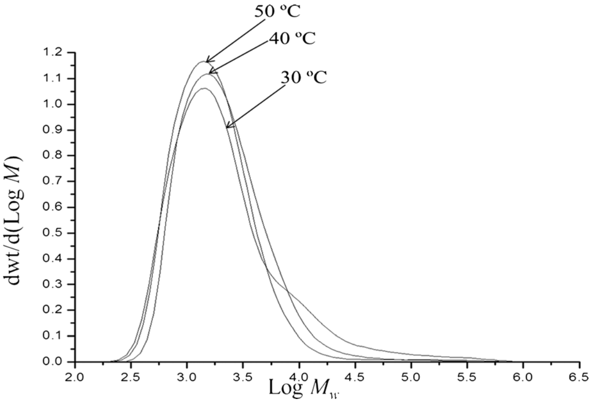

Figure 4. GPC traces of PE produced by MWCNT-**Fe2** at different temperatures (Table 2, Entries 9, 11, and 12).

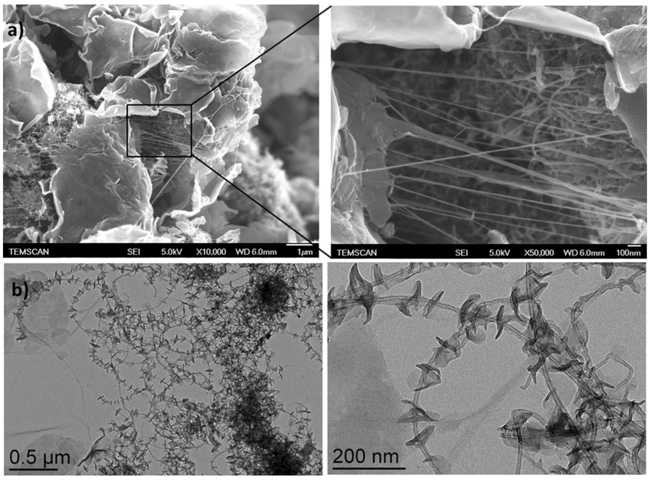

Figure 5. a) SEM images of MWCNT/PE composites; b) TEM images of the MWCNT/PE composites after partial removal of PE.

polymeric material is removed from the samples by dissolution, a particular lamellar structure is observed that shows a regular dispersion of small quantities of polymeric material along the MWCNTs (Figure 5 b), similar to that observed for the crystallization of PE around CNTs that act as nucleating agents.[23]

Conclusions

Two Fe complexes based on a 2,6-bis(imino)pyridyl framework that contain a pyrene moiety have been synthesized and characterized. Activated by modified methylaluminoxane, both Fe complex precatalysts promote ethylene polymerization with high activities, comparable to that of the most efficient systems described in the literature,[19a,c,d] which evidences a beneficial influence of the polyaromatic pyrene substituent(s) introduced on the ligands. By using π–π stacking interactions, catalysts supported on multiwalled carbon nanotubes (MWCNTs) are produced efficiently by impregnating the Fe complexes on the MWCNTs. Efficient anchoring is confirmed by IR spectroscopy, X-ray photoelectron spectroscopy, and inductively coupled plasma mass spectrometry. The catalytic screening of these heterogenized systems evidenced in one case a significant increase of the productivity compared to the analogous unsupported system, which has one pyrene moiety, whereas in another case, a lower production of polyethylene with a narrower polydispersity was obtained as a result of the presence of two pyrene moieties for interaction. This evidences the noninnocent role of the MWCNTs in the polymerization process. Finally, the resultant materials show a good dispersion of the MWCNTs into the polyethylene matrix, which results from the surface-initiated polymerization reaction.

Experimental Section

General considerations

All manipulations of air- and/or moisture-sensitive compounds were performed under a N_2 atmosphere by using standard Schlenk and glovebox techniques. Methylaluminoxane (MAO, 1.46 M solution in toluene) and modified methylaluminoxane (MMAO, 1.93 M in heptane, 3 A) were purchased from Akzo Nobel Corp.

High-purity ethylene was obtained from Beijing Yansan Petrochemical Co. $FeCl_2$, 1-aminopyrene, and 2,6-diacetylpyridine were purchased from Alfa Aesar. Multiwalled carbon nanotubes (MWCNT; 98% purity, 2% Fe catalyst, XRD: $d_{002}=0.3405$ nm, BET: 177 $m^2 g^{-1}$) were synthesized by chemical vapor deposition and purified according to previously reported procedures.[24] NMR spectra were recorded by using a Brucker AV 400 MHz instrument at ambient temperature using TMS as an internal standard. IR spectra were recorded by using a PerkinElmer spectra one spectrometer. Molecular weights (M_w) and the molecular weight distribution (M_w/M_n) of PEs were determined by gel-permeation chromatography (GPC) by using a PL-GPC220 instrument at 150 °C with 1,2,4-trichlorobenzene as the solvent. Differential scanning calorimetry (DSC) traces and the melting point of polyethylene were obtained from the second scanning run by using a PerkinElmer DSC-7 at a heating rate of 10 °C min^{-1}. X-ray photoelectron spectroscopy (XPS) measurements were performed by using a K-alpha Thermo Scientific instrument operating with an AlK_α source (1486.6 eV). The binding energies were corrected with respect to the C 1s core level fixed at 284.4 eV. ICP-MS measurements were performed at Antellis. SEM images were obtained on a JEOL JSM 6700 Field Emission Gun scanning electron microscope.

Synthesis and characterization

Synthesis of 2-[1-(2,6-diisopropylphenylimino)ethyl]-6-[1-(pyren-1-ylimino)ethyl]pyridine (L1)

The monoamine 2-[1-(2,6-diisopropylphenylimino)ethyl]-6-acetylpyridine (**A**) was synthesized by the condensation reaction of 2,6-diacetylpyridine with 2,6-diisopropylaniline according to a previously reported procedure.[25] A mixture of **A** (0.97 g, 3 mmol), 1-aminopyrene (1.5 equiv., 0.98 g, 4.5 mmol), and a catalytic amount of *p*-toluenesulfonic acid (0.1 g) in toluene (50 mL) was heated to reflux for 10 h. After solvent evaporation, the crude product was purified by column chromatography on silica gel with petroleum ether/ethyl acetate (50:1 v/v) as the eluent to afford **L1** as a yellow powder in 68% yield. IR (KBr): $\tilde{\nu}=3029$ (m), 1639 (s), 1597 (w), 1454 (m), 1362 (m), 1228 (m), 1105 (s), 840 (m), 765 cm^{-1} (m); ^1H NMR (400 MHz, [D$_6$]acetone, TMS): $\delta=8.72$ (dd, 1 H, $^3J=4.5$ Hz,

$^4J = 0.8$ Hz, pyridine), 8.59 (dd, 1H, $^3J = 4.4$ Hz, Py), 8.33 (d, 1H, $J = 4.1$ Hz, pyrene), 8.03- 8.28 (m, 8H, pyrene, Ar), 7.60 (d, 1H, $J = 4.1$ Hz, Ar), 7.22 (d, 2H, $J = 4.1$, Ar), 7.11 (t, 1H, $J = 4.5$ Hz, Ar), 2.83–2.91 (m, 2H, C*H*), 2.48 (s, 3H, CH_3), 2.33(s, 3H, CH_3), 1.16–1.22 ppm (m, 12H, CH(CH_3)$_2$); ^{13}C NMR (100 MHz, [D$_6$]acetone, TMS): $\delta =$ 165.4, 164.9, 148.2, 137.9, 137.4, 135.5, 131.8, 127.5, 126.9, 126.3, 125.9, 124.8, 124.6, 123.7, 123.6, 122.9, 122.8, 122.7, 122.6, 122.3, 22.6, 22.1, 16.5, 16.1 ppm.

Synthesis of 2,6-bis[1-(pyren-1-ylimino)ethyl]pyridine (L2)

A mixture of 2,6-diacetylpyridine (0.97 g, 2 mmol), 1-aminopyrene (3 equiv., 1.27 g, 6 mmol), and a catalytic amount of *p*-toluenesulfonic acid (0.1 g) in toluene (50 mL) was heated to reflux for 3 d. After solvent evaporation, the crude product was purified by column chromatography on silica gel with petroleum ether/ethyl acetate (50:1 v/v) as the eluent to afford **L2** as a yellow powder in 52% yield. IR (KBr): $\tilde{\nu} = 3045$ (m), 1638 (s), 1621 (m), 1566 (m), 1449 (w), 1362 (s), 1226 (s), 1119 (m), 848(s), 758 (s), 711 cm^{-1} (m); ^{1}H NMR (400 MHz, CDCl$_3$, TMS): $\delta = 8.72$ (d, 2H, $J = 3.8$ Hz, Py), 8.20 (d, 2H, $J = 4.0$ Hz, Py), 8.14–8.17 (m, 4H, Ar), 8.05–8.09 (m, 3H, Py H, Ar H), 8.04–8.07 (m, 6H, Ar), 8.03 (d, 2H, $J = 3.8$ Hz, Ar), 7.39 (d, 2H, $J = 4.0$ Hz, Ar), 2.36 ppm (s, 6H, CH_3); ^{13}C NMR (100 MHz, CDCl$_3$, TMS): $\delta = 168.8$, 155.5, 145.6, 137.2, 131.7, 131.5, 127.9, 127.4, 126.9, 126.1, 125.9, 125.4, 124.8, 124.6, 122.9, 122.8, 116.6, 17.0 ppm.

Synthesis of Fe1 and Fe2

The Fe complexes were prepared by the reaction of FeCl$_2$ with **L1** or **L2** (1 equiv.) in THF at RT for 12 h (Scheme 1). The obtained precipitate was collected by filtration, washed with diethyl ether, and dried under reduced pressure. **Fe1**: Yield: 88%; IR (KBr): $\tilde{\nu} = 1621$ (w), 1586 (s), 1463 (m), 1436 (m), 1371 (s), 1104 (m), 845 (s), 799 (m), 713 cm^{-1} (m); elemental analysis calcd (%) for $C_{37}H_{35}Cl_2FeN_3$ (647.16): C 68.53, H 5.44, N 6.48; found C 68.83, H 5.43, N 6.38. **Fe2**: Yield: 82%; IR (KBr): $\tilde{\nu} = 1623$ (w), 1586 (s), 1504 (w), 1486 (w), 1369 (m), 1265(m), 1186 (w), 843 (s), 710 cm^{-1} (m).

Immobilization of Fe complexes on MWCNTs

Prior to use, the MWCNTs were purified and cut. Under an N$_2$ atmosphere, CH$_2$Cl$_2$ (100 mL) was added to a mixture of MWCNTs (3 g) and **Fe1** or **Fe2** (0.15 g). The resulting suspension was stirred for 6 h at RT. After filtration, the black powder was fully washed by toluene and CH$_2$Cl$_2$ and then dried under vacuum for 2 d. The amount of Fe complex anchored on the MWCNT (2658 mg$_{Fe}$kg^{-1} for **Fe1** and 2909 mg$_{Fe}$kg^{-1} for **Fe2**) was determined by ICP-MS taking into account the amount of Fe present (residual catalyst) in the unfunctionalized samples.

X-ray crystallographic studies

Crystals of **Fe1** suitable for XRD analysis were obtained by layering diethyl ether onto a solution of **Fe1** in methanol at RT on a Rigaku Saturn724$^+$ CCD. With graphite-monochromated MoK$_\alpha$ radiation ($\lambda = 0.71073$ Å) at 173(2) K, cell parameters were obtained by global refinement of the positions of all collected reflections. Intensities were corrected for Lorentz and polarization effects and empirical absorption. The structures were solved by direct methods and refined by full-matrix least squares on F^2. All H atoms were placed in calculated positions. Structure solution and refinement were performed by using the SHELXL-97 package.[26] Details of the X-ray structure determinations and refinements are provided in Table 3. CCDC 951611 contains the supplementary crystallographic data for this paper. These data can be obtained free of charge from The Cambridge Crystallographic Data Centre via www.ccdc.cam.ac.uk/data_request/cif.

Table 3. Crystal data and structure refinement for **Fe1**.

Empirical formula	$C_{37}H_{35}Cl_2$ FeN_3
Formula weight	648.43
T [K]	173(2)
Wavelength [Å]	0.71073
Crystal system	Tetragonal
Space group	*I*4(1)/*a*
a [Å]	23.447(3)
b [Å]	23.447(3)
c [Å]	29.697(6)
α [°]	90
β [°]	90
γ [°]	90
V [Å^3]	16326(5)
Z, D_{calcd} [g cm^{-3}]	16, 1.055
μ [mm^{-1}]	1.345
F(000)	5408
Crystal size [mm]	0.17 × 0.03 × 0.03
θ range [°]	1.11–25.32
Limiting indices	$-13 \leq h \leq 28$
	$-15 \leq k \leq 28$
	$-35 \leq l \leq 24$
Reflections collected	15655
Independent reflections	7443, [*R*(int) = 0.0623]
Number of parameters	416
Completeness to θ [%]	99.8%
Goodness of fit on F^2	1.012
Final *R* indices [$I > 2\sigma(I)$]	$R1 = 0.0933$, $wR2 = 0.2243$
R indices (all data)	$R1 = 0.1547$, $wR2 = 0.2551$
Max./min. $\Delta\rho$[a] [eÅ^{-3}]	0.384 and −0.263

Procedure for ethylene polymerization

Homogeneous polymerization

Ethylene polymerization at 10 atm ethylene pressure was performed by using a 250 mL stainless-steel autoclave equipped with a mechanical stirrer and a temperature controller. Toluene, the desired amount of Fe precatalyst, and a toluene solution of the cocatalyst (to achieve a total volume of 100 mL) were added to the reactor in this order under an ethylene atmosphere. When the desired reaction temperature was reached, the ethylene pressure was increased to 10 atm, and maintained at this level by a constant feed of ethylene. After the desired reaction time, the reaction was quenched by addition of acidic ethanol. The precipitated polymer was washed with ethanol and water several times and dried in vacuum.

Polymerization using the MWCNT-supported Fe complexes

Heterogeneous polymerizations were performed by first adding MWCNT-supported catalyst (0.05 g) into the reactor. Then toluene and the desired amount of cocatalyst (to achieve a total volume of 100 mL) were added to the reactor under an ethylene atmosphere. The following procedure was the same as that used for homogeneous polymerization.

Acknowledgements

This work was supported by NSFC No. 20911130359 and ANR No. ANR-09-BLAN-0384.

Keywords: carbon nanotubes · immobilization · iron · polymerization · supported catalysts

[1] M. F. L. De Volder, S. H. Tawfick, R. H. Baughman, A. J. Hart, *Science* **2013**, *339*, 535 – 539.

[2] a) E. Castillejos, P.-J. Debouttière, L. Roiban, A. Solhy, V. Martinez, Y. Kihn, O. Ersen, K. Philippot, B. Chaudret, P. Serp, *Angew. Chem. Int. Ed.* **2009**, *48*, 2529 – 2533; *Angew. Chem.* **2009**, *121*, 2567 – 2571; b) P. Serp, E. Castillejos, *ChemCatChem* **2010**, *2*, 41 – 47; c) M. Escárcega-Bobadilla, L. Rodríguez-Pérez, E. Teuma, P. Serp, A. Masdeu-Bultó, M. Gómez, *Catal. Lett.* **2011**, *141*, 808 – 816; d) A. Schaetz, M. Zeltner, W. J. Stark, *ACS Catal.* **2012**, *2*, 1267 – 1284; e) D. S. Su, S. Perathoner, G. Centi, *Chem. Rev.* **2013**, *113*, 5782 – 5816.

[3] a) S. Banerjee, S. S. Wong, *J. Am. Chem. Soc.* **2002**, *124*, 8940 – 8948; b) Y. Liu, A. Adronov, *Macromolecules* **2004**, *37*, 4755 – 4760; c) L. Lemus-Yegres, I. Suchbasanez, C. Delecea, P. Serp, M. Romanmartinez, *Carbon* **2006**, *44*, 605 – 608; d) W. Lu, N. Li, W. Chen, Y. Yao, *Carbon* **2009**, *47*, 3337 – 3345; e) G. Liu, B. Wu, J. Zhang, X. Wang, M. Shao, J. Wang, *Inorg. Chem.* **2009**, *48*, 2383 – 2390; f) S. Tangestaninejad, M. Moghadam, V. Mirkhani, I. Mohammadpoor-Baltork, M. S. Saeedi, *Appl. Catal. A* **2010**, *381*, 233 – 241; g) P. D. Tran, A. Le Goff, J. Heidkamp, B. Jousselme, N. Guillet, S. Palacin, H. Dau, M. Fontecave, V. Artero, *Angew. Chem. Int. Ed.* **2011**, *50*, 1371 – 1374; *Angew. Chem.* **2011**, *123*, 1407 – 1410; h) C. Costabile, F. Grisi, G. Siniscalchi, P. Longo, M. Sarno, D. Sannino, C. Leone, P. Ciambelli, *J. Nanosci. Nanotechnol.* **2011**, *11*, 10053 – 10062; i) S. Lee, J. Y. Shin, S.-g. Lee, *Tetrahedron Lett.* **2013**, *54*, 684 – 687; j) M. Blanco, P. Álvarez, C. Blanco, M. V. Jiménez, J. Fernández-Tornos, J. J. Pérez-Torrente, L. A. Oro, R. Menéndez, *ACS Catal.* **2013**, *3*, 1307 – 1317; k) D. Didier, E. Schulz, *Tetrahedron: Asymmetry* **2013**, *24*, 769 – 775; l) H. Sharghi, S. Ebrahimpourmoghaddam, M. M. Doroodmand, *J. Organomet. Chem.* **2013**, *738*, 41 – 48; m) H. Kargar, M. Moghadam, V. Mirkhani, S. Tangestaninejad, I. Mohammadpoor-Baltork, S. Rezaei, *Transition Met. Chem.* **2013**, *38*, 1 – 5; n) C. Vriamont, M. Devillers, O. Riant, S. Hermans, *Chem. Eur. J.* **2013**, *19*, 12009 – 12017.

[4] a) D. Bonduel, M. L. Mainil, M. L. Alexandre, F. Monteverde, P. Dubois, *Chem. Commun.* **2005**, 781 – 783; b) Y. Sánchez, C. Albano, A. Karam, R. Perera, E. Casas, *Macromol. Symp.* **2009**, *282*, 185 – 191.

[5] a) S. Park, S. W. Yoon, K.-B. Lee, D. J. Kim, Y. H. Jung, Y. Do, H.-j. Paik, I. S. Choi, *Macromol. Rapid Commun.* **2006**, *27*, 47 – 50; b) B. Choi, J. Lee, S. Lee, J. H. Ko, K. S. Lee, J. Oh, J. Han, Y. H. Kim, I. S. Choi, S. Park, *Macromol. Rapid Commun.* **2013**, *34*, 533 – 538.

[6] S. Park, I. S. Choi, *Adv. Mater.* **2009**, *21*, 902 – 905.

[7] B. M. Amoli, S. A. A. Ramazani, H. Izadi, *J. Appl. Polym. Sci.* **2012**, *125*, E453 – E461.

[8] L. Zhang, E. Yue, B. Liu, P. Serp, C. Redshaw, W.-H. Sun, J. Durand, *Catal. Commun.* **2014**, *43*, 227 – 230.

[9] a) X. Tong, C. Liu, H.-M. Cheng, H. Zhao, F. Yang, X. Zhang, *J. Appl. Polym. Sci.* **2004**, *92*, 3697 – 3700; b) M. Trujillo, M. L. Arnal, A. J. Müller, E. Laredo, S. Bredeau, D. Bonduel, P. Dubois, *Macromolecules* **2007**, *40*, 6268 – 6276; c) S. Park, S. W. Yoon, H. Choi, J. S. Lee, W. K. Cho, J. Kim, H. J. Park, W. S. Yun, C. H. Choi, Y. Do, I. S. Choi, *Chem. Mater.* **2008**, *20*, 4588 – 4594; d) S. Li, H. Chen, D. Cui, J. Li, Z. Zhang, Y. Wang, T. Tang, *Polym. Compos.* **2010**, *31*, 507 – 515; e) W. Kaminsky, A. Funck, H. Hahnsen, *Dalton Trans.* **2009**, 8803 – 8810; f) M. J. Go, S. H. Kim, K. M. Lee, H. H. Lee, H.-R. Park, J. Lee, S. Park, I. S. Choi, Y. Kim, *Polymer* **2012**, *53*, 933 – 938.

[10] a) B. L. Small, M. Brookhart, *J. Am. Chem. Soc.* **1998**, *120*, 7143 – 7144; b) B. L. Small, M. Brookhart, *Macromolecules* **1999**, *32*, 2120 – 2130; c) S. D. Ittel, L. K. Johnson, M. Brookhart, *Chem. Rev.* **2000**, *100*, 1169 – 1204.

[11] a) G. J. P. Britovsek, V. C. Gibson, S. J. McTavish, G. A. Solan, A. J. P. White, D. J. Williams, G. J. P. Britovsek, B. S. Kimberley, P. J. Maddox, *Chem. Commun.* **1998**, *0*, 849 – 850; b) G. J. P. Britovsek, M. Bruce, V. C. Gibson, B. S. Kimberley, P. J. Maddox, S. Mastroianni, S. J. McTavish, C. Redshaw, G. A. Solan, S. Strömberg, A. J. P. White, D. J. Williams, *J. Am. Chem. Soc.* **1999**, *121*, 8728 – 8740; c) G. J. P. Britovsek, V. C. Gibson, D. F. Wass, *Angew. Chem. Int. Ed.* **1999**, *38*, 428 – 447; *Angew. Chem.* **1999**, *111*, 448 – 468; d) V. C. Gibson, S. K. Spitzmesser, *Chem. Rev.* **2003**, *103*, 283 – 316.

[12] a) V. C. Gibson, C. Redshaw, G. A. Solan, *Chem. Rev.* **2007**, *107*, 1745 – 1776; b) C. Bianchini, G. Giambastiani, L. Luconi, A. Meli, *Coord. Chem. Rev.* **2010**, *254*, 431 – 455; c) W. Zhang, W.-H. Sun, C. Redshaw, *Dalton Trans.* **2013**, *42*, 8988 – 8997.

[13] a) Z. Ma, W.-H. Sun, Z.-L. Li, C.-X. Shao, Y.-L. Hu, X.-H. Li, *Polym. Int.* **2002**, *51*, 994 – 997; b) Y. Chen, C. Qian, J. Sun, *Organometallics* **2003**, *22*, 1231 – 1236; c) B. L. Small, M. J. Carney, D. M. Holman, C. E. O'Rourke, J. A. Halfen, *Macromolecules* **2004**, *37*, 4375 – 4386; d) F. Pelascini, M. Wesolek, F. Peruch, P. J. Lutz, *Eur. J. Inorg. Chem.* **2006**, 4309 – 4316; e) F. A. R. Kaul, G. T. Puchta, G. D. Frey, E. Herdtweck, W. A. Herrmann, *Organometallics* **2007**, *26*, 988 – 999; f) C. Wallenhorst, G. Kehr, H. Luftmann, R. Fröhlich, G. Erker, *Organometallics* **2008**, *27*, 6547 – 6556; g) L.-h. Guo, H.-y. Gao, L. Zhang, F.-m. Zhu, Q. Wu, *Organometallics* **2010**, *29*, 2118 – 2125; h) W. Zhao, J. Yu, S. Song, W. Yang, H. Liu, X. Hao, C. Redshaw, W.-H. Sun, *Polymer* **2012**, *53*, 130 – 137; i) S. Blanchard, E. Derat, M. Desage-El Murr, L. Fensterbank, M. Malacria, V. Mouriès-Mansuy, *Eur. J. Inorg. Chem.* **2012**, 376 – 389.

[14] a) F. A. R. Kaul, G. T. Puchta, H. Schneider, F. Bielert, D. Mihalios, W. A. Herrmann, *Organometallics* **2002**, *21*, 74 – 82; b) I. S. Paulino, U. Schuchardt, *Catal. Commun.* **2004**, *5*, 5 – 7; c) J. R. Severn, J. C. Chadwick, R. Duchateau, N. Friederichs, *Chem. Rev.* **2005**, *105*, 4073 – 4147; d) L. Beaufort, F. Benvenuti, A. F. Noels, *J. Mol. Catal. A* **2006**, *260*, 215 – 220.

[15] a) G. Leone, F. Bertini, M. Canetti, L. Boggioni, L. Conzatti, I. Tritto, *J. Polym. Sci. Part A* **2009**, *47*, 548 – 564; b) B. Bahuleyan, J. Oh, D. Chandran, J. Ha, A. Hur, D.-W. Park, C. Ha, H. Suh, I. Kim, *Top. Catal.* **2010**, *53*, 500 – 509.

[16] N. Karousis, N. Tagmatarchis, D. Tasis, *Chem. Rev.* **2010**, *110*, 5366 – 5397.

[17] A. Hirsch, O. Vostrowsky in *Functional Molecular Nanostructures, Vol. 245* (Ed.: A. D. Schlüter), Springer, Berlin, **2005**, pp. 193 – 237.

[18] X. Peng, S. S. Wong, *Adv. Mater.* **2009**, *21*, 625 – 642.

[19] a) G. S. Machado, K. A. Dias de Freitas Castro, F. Wypych, S. Nakagaki, *J. Mol. Catal. A* **2008**, *283*, 99 – 107; b) Z. Zhang, C. H. Turner, *J. Phys. Chem. C* **2013**, *117*, 8758 – 8766; c) R. Cao, R. Thapa, H. Kim, X. Xu, M. Gye Kim, Q. Li, N. Park, M. Liu, J. Cho, *Nat. Commun.* **2013**, *4*, 2076 – 2082.

[20] a) J. Yu, H. Liu, W. Zhang, X. Hao, W.-H. Sun, *Chem. Commun.* **2011**, *47*, 3257 – 3259; b) W.-H. Sun, W. Zhao, J. Yu, W. Zhang, X. Hao, C. Redshaw, *Macromol. Chem. Phys.* **2012**, *213*, 1266 – 1273; c) X. Cao, F. He, W. Zhao, Z. Cai, X. Hao, T. Shiono, C. Redshaw, W.-H. Sun, *Polymer* **2012**, *53*, 1870 – 1880; d) S. Wang, B. Li, T. Liang, C. Redshaw, Y. Li, W.-H. Sun, *Dalton Trans.* **2013**, *42*, 9188 – 9197; e) W. Zhang, W. Chai, W.-H. Sun, X. Hu, C. Redshaw, X. Hao, *Organometallics* **2012**, *31*, 5039 – 5048.

[21] G. J. P. Britovsek, S. Mastroianni, G. A. Solan, S. P. D. Baugh, C. Redshaw, V. C. Gibson, A. J. P. White, D. J. Williams, M. R. J. Elsegood, *Chem. Eur. J.* **2000**, *6*, 2221 – 2231.

[22] a) K. V. Singh, R. R. Pandey, X. Wang, R. Lake, C. S. Ozkan, K. Wang, M. Ozkan, *Carbon* **2006**, *44*, 1730 – 1739; b) O. O. Ogunro, X.-Q. Wang, *New J. Chem.* **2010**, *34*, 1084 – 1088; c) A. K. Manna, S. K. Pati, *Nanoscale* **2010**, *2*, 1190 – 1195.

[23] E. D. Laird, C. Y. Li, *Macromolecules* **2013**, *46*, 2877 – 2891.

[24] a) M. Corrias, B. Caussat, A. Ayral, J. Durand, Y. Kihn, P. Kalck, P. Serp, *Chem. Eng. Sci.* **2003**, *58*, 4475 – 4482; b) R. Philippe, A. Morançais, M. Corrias, B. Caussat, Y. Kihn, P. Kalck, D. Plee, P. Gaillard, D. Bernard, P. Serp, *Chem. Vap. Deposition* **2007**, *13*, 447 – 457; c) A. Solhy, B. F. Machado, J. Beausoleil, Y. Kihn, F. Gonçalves, M. F. R. Pereira, J. J. M. Órfão, J. L. Figueiredo, J. L. Faria, P. Serp, *Carbon* **2008**, *46*, 1194 – 1207.

[25] C. Bianchini, G. Mantovani, A. Meli, F. Migliacci, F. Zanobini, F. Laschi, A. Sommazzi, *Eur. J. Inorg. Chem.* **2003**, 1620 – 1631.

[26] G. M. Sheldrick, SHELXTL-97, Program for the Refinement of Crystal Structures, University of Göttingen, Germany, **1997**.

Received: December 11, 2013